Physics Letters B 744 (2015) 268–272

Contents lists available at ScienceDirect

Physics Letters B

www.elsevier.com/locate/physletb

Galactic production of ^{138}La: Impact of ^{138,139}La statistical properties

B.V. Kheswa [a,b,*], M. Wiedeking [a], F. Giacoppo [c], S. Goriely [d], M. Guttormsen [c], A.C. Larsen [c], F.L. Bello Garrote [c], T.K. Eriksen [c], A. Görgen [c], T.W. Hagen [c], P.E. Koehler [c], M. Klintefjord [c], H.T. Nyhus [c], P. Papka [b], T. Renstrøm [c], S. Rose [c], E. Sahin [c], S. Siem [c], T. Tornyi [c]

[a] iThemba LABS, P.O. Box 722, 7129 Somerset West, South Africa
[b] Physics Department, University of Stellenbosch, Private Bag X1, Matieland 7602, Stellenbosch, South Africa
[c] Department of Physics, University of Oslo, N-0316 Oslo, Norway
[d] Institut d'Astronomie et d'Astrophysique, Université Libre de Bruxelles, CP 226, B-1050 Brussels, Belgium

ARTICLE INFO

Article history:
Received 17 November 2014
Received in revised form 12 February 2015
Accepted 31 March 2015
Available online 2 April 2015
Editor: D.F. Geesaman

Keywords:
γ-ray strength functions
Nuclear level densities
Maxwellian averaged cross-sections

ABSTRACT

The γ-ray strength functions and nuclear level densities of ^{138}La and ^{139}La have been measured below the neutron separation energies. These new data were used to calculate astrophysical Maxwellian-averaged (n,γ) cross-sections to investigate the production and destruction of the p-nucleus ^{138}La in the photodisintegration process. The results confirm the underproduction of ^{138}La in the p-process with respect to the observed abundances and strongly support the ν-process through ν_e capture on ^{138}Ba as the main contributor to the synthesis of ^{138}La in Type II supernovae.

1. Introduction

The major mechanisms to explain the synthesis of nuclei heavier than iron in the universe are: (a) the slow neutron-capture process (s-process), which occurs during the hydrostatic stellar burning phases of low-mass stars during their asymptotic giant branch phase [1] or of massive stars during core He-burning; (b) the rapid neutron-capture process (r-process) taking place in extremely high-neutron density environments [2]. The astrophysical sources and the specific conditions in which the r-process takes place are among the most longstanding mysteries of nuclear astrophysics. While the light r-process elements up to the first (or possibly second) abundance peak might be produced in neutrino-driven outflows of core-collapse supernovae [3–5], the decompression of cold neutronized matter from the violent collision of binary neutron stars or a neutron star with companion black holes have also been suggested as alternative sites [2,6–8].

Neutron capture processes can generally explain isotopic abundances with the notable exception of 35 p-nuclei which are stable or very long-lived systems with half-lives on the order of Gyr. Their production through the s- or r-processes is prohibited and they are instead synthesized in the p-process through photodisintegration reactions, i.e. (γ,n), (γ,p) or (γ,α), originating from seed nuclei which are created by the s- or r-processes [9] instead. The p-process can explain the observed solar abundances of most p-nuclei, with a few exceptions, one of them being ^{138}La [9–14]. ^{138}La is shielded from beta decay contributions by the stable isobars ^{138}Ce and ^{138}Ba, and photoreactions appear to be inefficient to produce ^{138}La significantly. The most promising theory brought forward for the synthesis of ^{138}La suggests that neutrinos from the proto-neutron star, created following the core-collapse, have enough intensity and energy to interact with matter through neutrino-induced reactions [13,15]. In particular the ^{138}Ba ν_e-capture has been calculated to be the largest contributor in the production of ^{138}La [10].

However, it was also clearly pointed out that nuclear physics properties, such as the nuclear level density (NLD) and γ-ray strength function (γSF), which are important ingredients in reaction rate calculations, are the main sources of uncertainty to evaluate the efficiency of the standard p-process mechanism [10]. The production of ^{138}La through ^{139}La$(\gamma,n)^{138}$La and its destruction by ^{138}La$(\gamma,n)^{137}$La are exclusively based on theoretical predictions. The NLD and γSF have never been measured for ^{138}La below the particle separation energy (S_n), which is the primary energy region of importance in the synthesis of ^{138}La. Data for ^{139}La are only available for excitation energies above 6 MeV [16]. Nuclear

* Corresponding author at: iThemba LABS, P.O. Box 722, 7129 Somerset West, South Africa.
E-mail address: bngkheswa@gmail.com (B.V. Kheswa).

http://dx.doi.org/10.1016/j.physletb.2015.03.065

physics parameters and their uncertainties need to be carefully measured in order to use them in model calculations to unambiguously exclude the standard p-process as the main contributor, and to confidently discuss the importance of neutrino interactions in the production of ^{138}La.

In this Letter, we report the measurements of the γSF and NLD in ^{138}La and ^{139}La below S_n. These experimental results are subsequently used in reaction rate calculations to determine their impact on the observed abundances. The implications for the p- and ν_e-processes in the synthesis of ^{138}La will be addressed.

2. Experimental results

The seven-day experiment was conducted at the Oslo Cyclotron Laboratory with a ^{3}He beam of 38 MeV impinging on a 2.5 mg/cm^2 thick ^{139}La (99.9%) target. The beam intensity was kept in the range ≈0.4–0.7 pnA. Excited states in ^{138}La and ^{139}La nuclei were populated in the ^{139}La(^{3}He, ^{4}He) and ^{139}La(^{3}He, ^{3}He′) reactions, respectively. Particles and γ-rays were measured in coincidence using the CACTUS (26 5″ × 5″ NaI detectors) and SiRi (64 ΔE–E telescopes with 130 μm thick ΔE and 1550 μm thick E detectors) arrays [17,18]. CACTUS is mounted on a spherical frame such that the target is located at the center with a distance of 22 cm from each NaI detector. The SiRi array was placed downstream, 50 mm from the target and covers a mean scattering angular range of 40–54°. During the analysis only the range 40–52° was used. The total efficiency and resolution of the CACTUS array are 14.1% and 7% FWHM for a 1332 keV transition, respectively. The particle telescopes have a resolution of ≈260 keV for the ^{3}He elastic peak. A 10.5 μm thick Al foil covers the front side of the particle telescopes to suppress δ-electrons.

The NaI detectors were calibrated with the 780.9 keV and 2759.1 keV γ-ray transitions in ^{27}Si which were produced in the ^{28}Si(^{3}He, ^{4}He)^{27}Si reaction. The excitation energy, E_x, of the ^{138}La and ^{139}La nuclei were obtained from the measured total energy of the ^{4}He and ^{3}He particles, corrected for kinematic effects, energy losses, and different Q-values. The particle-γ coincidence window was set to ≈50 ns by gating on the prompt time peak.

The Oslo Method [19,20] was used to extract the γSF and NLD simultaneously. The E_x vs. E_γ matrices were constructed individually for ^{138}La and ^{139}La and have been unfolded with the CACTUS response matrix and the iterative technique discussed in [21]. The first generation matrices, $P(E_x, E_\gamma)$, were extracted (see Fig. 1) using the first generation method [22]. This iterative subtraction procedure reveals the distribution of the primary γ-rays for each initial excitation energy bin. The diagonal valley without data in Fig. 1(b) corresponds to the 1043 keV energy difference between the first- and second-excited states of ^{139}La. In the same figure two vertical regions corresponding to $E_\gamma \approx 1$ and 1.7 MeV are visible which are characterized by lower statistics due to over-subtraction of discrete and strong γ-ray transitions during the generation of $P(E_x, E_\gamma)$.

The NLD and γSF are obtained from $P(E_x, E_\gamma)$ for both La nuclei under study. Assuming that the residual nucleus reaches a compound-like state before γ emission [23], and the Brink Hypothesis [24] is valid, $P(E_x, E_\gamma)$ can be factorized as [19],

$$P(E_x, E_\gamma) \propto \tilde{\rho}(E_f)\tilde{\mathcal{T}}(E_\gamma), \tag{1}$$

where $\tilde{\mathcal{T}}(E_\gamma)$ and $\tilde{\rho}(E_f)$ are the γ-ray transmission coefficient and level density at $E_f = E_x - E_\gamma$, respectively. Values for $\tilde{\mathcal{T}}(E_\gamma)$ and $\tilde{\rho}(E_f)$ were extracted by fitting theoretical first-generation matrices, $P_{th}(E_x, E_\gamma)$, to the experimental first-generation matrices $P(E_x, E_\gamma)$ individually for ^{138}La and ^{139}La. A χ^2 minimization between $P_{th}(E_x, E_\gamma)$ and $P(E_x, E_\gamma)$ using an iterative procedure

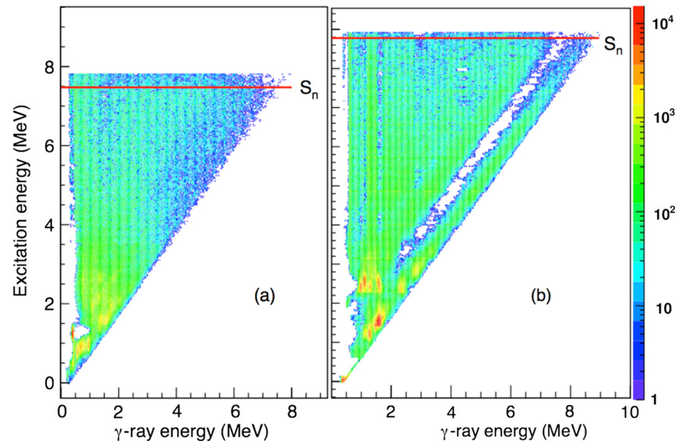

Fig. 1. (Color online.) The first-generation matrices, $P(E_x, E_\gamma)$, for ^{138}La (a) and ^{139}La (b). The neutron separation energies, S_n, are indicated by horizontal lines.

Table 1
Parameters used for the normalization of $\rho(E_x)$ and $f(E_\gamma)$ in ^{138,139}La.

Isotope	σ	D_0 (eV)	$\rho(S_n)$ (10^5 MeV^{-1})	$\langle\Gamma_\gamma(S_n)\rangle$ (meV)
^{138}La	6.9 ± 0.7 [a]	20.0 ± 4.4 [b]	7.1 ± 1.9 [b]	71.0 ± 13.6 [b]
^{139}La	5.5 ± 0.6 [a]	31.8 ± 7.0 [c]	2.9 ± 0.6 [a]	95.0 ± 18.2 [c]

[a] Calculated with the HFB + Combinatorial model [25].
[b] Estimated values (see text for details).
[c] Average value from Refs. [28,29].

[19] determines the best fit, which was performed in the energy regions of $E_\gamma \geq 1$ MeV and 3.5 MeV $\leq E_x \leq 7.1$ MeV for ^{138}La, and $E_\gamma \geq 1.7$ MeV and 3.5 MeV $\leq E_x \leq 8.5$ MeV for ^{139}La, to exclude the non-statistical excitation energy regions.

Following extraction of $\tilde{\mathcal{T}}(E_\gamma)$ and $\tilde{\rho}(E_f)$, infinitely many solutions of $P(E_x, E_\gamma)$ can be found of the form,

$$\rho(E_f) = \tilde{\rho}(E_f)Ae^{\alpha E_f} \tag{2}$$

$$\mathcal{T}(E_\gamma) = \tilde{\mathcal{T}}(E_\gamma)Be^{\alpha E_\gamma} \tag{3}$$

where α is the common slope for $\rho(E_f)$ and $\mathcal{T}(E_\gamma)$ and A and B are normalization parameters. Determination of α and A is accomplished by normalizing $\rho(E_f)$ to the level density at the neutron separation energy, $\rho(S_n)$, and at low excitation energies to the density of known discrete states. For ^{139}La, $\rho(S_n) = 2.9 \pm 0.6 \times 10^5$ MeV^{-1}, was used for normalization and was calculated from the experimental average neutron resonance level spacing, D_0 (see Table 1), using the Hartree–Fock–Bogoliubov (HFB) plus combinatorial model [25]. This value is in excellent agreement with $\rho(S_n) = 2.5 \pm 0.6 \times 10^5$ MeV^{-1} from the back shifted Fermi gas approach [26]. The absolute normalization parameter B is calculated using [20]:

$$\langle\Gamma_\gamma(S_n, J_T \pm \frac{1}{2}, \pi_T)\rangle = \frac{D_0}{4\pi}\int_0^{S_n} dE_\gamma \mathcal{T}(E_\gamma)\rho(S_n - E_\gamma) \times \sum_{J=-1}^{1} g(S_n - E_\gamma, J_T \pm \frac{1}{2} + J) \tag{4}$$

where J_T, π_T are the spin and parity of the target nucleus in the (n, γ) reactions and $g(S_n - E_\gamma, J_T \pm \frac{1}{2} + J)$ is the spin distribution [20,27] which is normalized to $\sum_J g(E_x, J) \approx 1$. For ^{139}La $\langle\Gamma_\gamma(S_n, J_T, \pi_T)\rangle$, and D_0 are available experimental values, and averaged from Refs. [28,29]. Their respective uncertainties were obtained with appropriate error propagation. However, for ^{138}La